Interface-Engineered Junctions With YbBaCuO as the Counter-Electrode

Jiro Yoshida, Hiroshi Katsuno, Kohei Nakayama, Shinji Inoue, and Toshihiko Nagano

***Abstract*—The electric properties of interface-engineered junctions with $YbBa_2Cu_3O_7$ as the counter-electrode were investigated. The junctions exhibited excellent Josephson characteristics with the critical current density (J_c) ranging from 10^2 A/cm^2 to more than 10^6 A/cm^2, and the normal resistance (R_n) ranging from 10^{-6} Ωcm^2 to 10^{-9} Ωcm^2. The R_n values varied approximately in accordance with J_c^{-p}, where p was close to 0.25 for low-J_c junctions and increased gradually up to 0.75 for high-J_c junctions. The junctions with R_n exceeding 10^{-7} Ωcm^2 exhibited dI/dV profiles peculiar to tunneling processes via localized states. The dI/dV profiles of the junctions with lower R_n were characterized by reproducible fine structures below 15 mV, probably due to multiple Andreev reflections. These results indicate that the crossover from the tunneling regime to metallic weak-links takes place in these junctions depending on the process conditions.**

***Index Terms*—Andreev reflection, interface-engineered junction, Josephson junction, tunneling.**

I. Introduction

Interface-engineered junctions (IEJ's) are regarded as the most promising candidates for high-T_c digital circuit applications as they are superior to other high-T_c Josephson junctions in terms of uniformity and reproducibility [1]–[3]. However, the electrical properties of IEJ's are sensitive to the substrate temperature for the counter-electrode deposition, and the I_c value appropriate for single flux quantum (SFQ) circuits can be obtained only in a low substrate temperature range. This temperature range sometimes conflicts with the requirement for the complete c-axis orientated growth of the counter-electrode layer with minimum sheet inductance L_s, especially when sputter-deposited $YBa_2Cu_3O_7$ (YBCO) is utilized as the counter electrode.

Recently, we reported that this trade-off between I_c and L_s could be solved by adopting $YbBa_2Cu_3O_7$ (YbBCO) as the counter-electrode, because it can grow with complete c-axis orientation in a far wider temperature range than is possible with other 123 compounds [3]. Those junctions with a completely c-axis-oriented YbBCO counter electrode exhibited excellent Josephson characteristics with the 1 σ-spread in I_c of 5.4% for 16 junctions with an average I_c of around 1 mA at 4.2 K.

Manuscript received August 5, 2002. This work was supported by the New Energy and Industrial Technology Development Organization (NEDO) through ISTEC as Collaborative Research and Development of Fundamental Technologies for Superconductivity Applications.

The authors are with the Advanced Materials and Devices Laboratory, Corporate Research and Development Center, Toshiba Corporation, Kawasaki 212-8582, Japan (e-mail: jiro-yoshida@arl.rdc.toshiba.co.jp).

Digital Object Identifier 10.1109/TASC.2003.813958

In spite of such progress in the fabrication technology, neither the structure of the barrier nor the current transport mechanism in IEJ's is well understood. Reliable experimental data on the current transport in IEJ's is highly desired not only for promoting the understanding of the junction physics but also to find a way to further reduce the 1σ-spreads in I_c values.

II. Fabrication Process

IEJ's with YbBCO as the counter-electrode were fabricated on ramp-edges formed in 200-nm thick YBCO base-electrode layers. An epitaxial $SrTiO_3$, CeO_2, or $SrSnO_3$ film was used for the interlayer isolation. We have not observed any significant difference in junction characteristics among junctions with different isolation layers. All the films used in the present work were grown on $SrTiO_3$ (100) substrates using an off-axis sputtering system.

Ramp-edge structures were produced using a photoresist mask reflowed after patterning, together with Ar-ion milling with substrate rotation during etching. The resultant ramp edges had a taper of 20 degrees independent of the edge orientation in a wafer. After etching, the samples were heated to the temperature for the subsequent layer deposition and maintained at that temperature for 10 minutes. An activated oxygen flux from an ECR plasma source was supplied during this annealing process. Then, a 300-nm thick YbBCO layer was deposited and the counter-electrode pattern was formed after covering the wafer surface with a 1-μm thick Au film. The junction width was fixed at 4 μm throughout the present work.

Empirically, we know that the junction characteristics are sensitive to the substrate temperature for the counter-electrode deposition and the power supplied to the ECR plasma source during the annealing process. Other factors that have significant influence on the junction characteristics are the acceleration voltage and the incident angle of the Ar-ion beam utilized for the fabrication of the ramp-edge structure. By varying these process parameters, we have obtained IEJ's with a Josephson critical current density (J_c) ranging from 10^2 to 10^6 A/cm^2. From among the large number of junctions, only those exhibiting excellent Josephson characteristics with a magnetic field modulation of I_c exceeding 75% at 4.2 K were selected for detailed investigation.

III. Junction Characteristics

Fig. 1 depicts an example of the current-voltage (I–V) characteristics observed at 4.2 K for an IEJ with a critical current density amounting to 4.5×10^5 A/cm^2. The pale line represents the I–V curve in a magnetic field of 7.4×10^3 A/m applied parallel to the junction interface. It is apparent that the I–V charac-

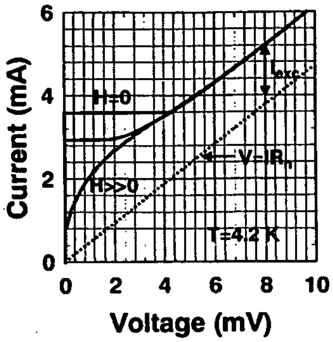

Fig. 1. Current-voltage characteristics observed at 4.2 K for an IEJ with a J_c of 4.5×10^5 A/cm^2 with and without an applied magnetic field which minimizes the zero-voltage current. The broken line represents simple ohmic behavior for reference.

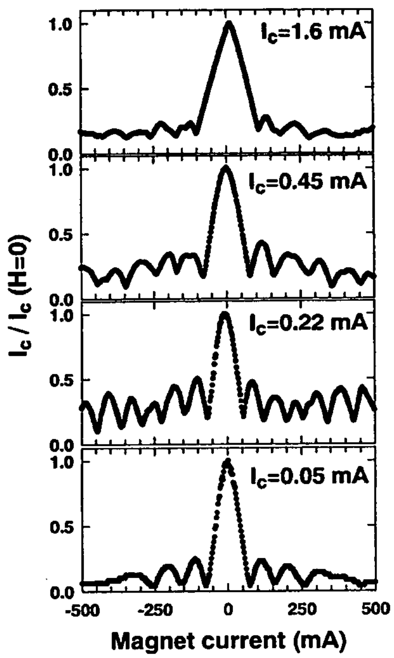

Fig. 2. Magnetic modulation of I_c observed for IEJ's with various Josephson critical currents. The crossover from small junction behavior to large junction behavior is seen between I_c = 0.5 mA and 1 mA.

teristics contain a large amount of excess current (I_{exc}) at high voltages. The excess current grows rapidly within an approximate voltage range of less than 5 mV, being accompanied by a weak bump-like structure within this voltage range. We also found that I_{exc}/I_c varied approximately in proportion to I_c for junctions with I_c exceeding 0.5 mA, and amounted to 30% for a junction with $I_c \sim 7$ mA. Such behavior seems to be consistent with the observation by Sydow *et al.* for their ozone-annealed IEJ's [4]. All these experimental results indicate that the excess current is not entirely due to the flux-flow behavior of the accidental microshorts in the junction but has close relation to Josephson characteristics.

Fig. 2 shows the magnetic field dependences of I_c observed at 4.2 K. The magnetic field modulation of I_c is almost 100% for low-I_c junctions, and is more than 80% even for a junction with I_c far exceeding 1 mA. In Fig. 2, we can see the crossover

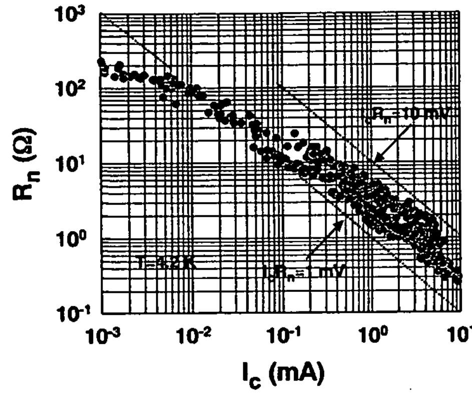

Fig. 3. Correlation between R_n and I_c observed for IEJ's processed under various conditions. R_n varies approximately in accordance with I_c^{-p} with p ranging from 0.25 to 0.75 depending on I_c. Variation in R_n with a factor of 3–4 is seen for junctions with similar I_c values in the high I_c region.

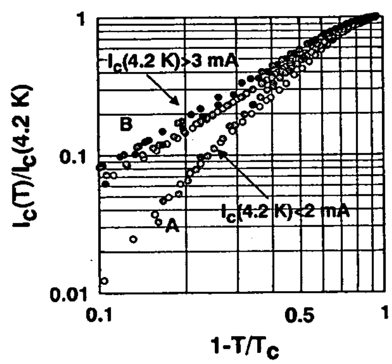

Fig. 4. Normalized I_c versus temperature characteristics for several junctions with different I_c values. The temperature dependence can be classified into two groups with an I_c at 4.2 K of 2–3 mA as the borderline.

from a small junction behavior to a large junction one by increasing the I_c value. The crossover takes place at I_c between 0.5 mA and 1 mA, which seems to be consistent with the London penetration depth of around 0.2 μm in high-T_c superconductors at 4.2 K.

Fig. 3 displays the correlation between the junction resistance (R_n) and I_c obtained for junctions on various wafers processed under various conditions. We defined the R_n value as the differential resistance within a current level of two to three times I_c. It can be seen that R_n varies approximately in accordance with I_c^{-p}, where p is close to 0.25 for junctions with an extremely small I_c value and is about 0.75 for junctions with $I_c > 1$ mA.

Another interesting point we can see in Fig. 3 is the large variation in R_n for junctions with similar I_c in the high I_c region. If we look at the junctions with I_c of 1 mA, we notice that the R_n value ranges from 1.3 to 5 Ω. Such variation in R_n is certainly beyond any experimental error, and suggests that the critical factors that influence I_c and R_n are not completely identical.

Fig. 4 shows the temperature dependences of I_c observed for several junctions with different I_c and R_n values. We found that the I_c versus temperature characteristics of our junctions could be classified into two groups with an I_c of 2–3 mA at 4.2 K as the borderline. Junctions with I_c smaller than 2 mA are characterized by their $(1 - T/T_c)^2$ dependence near T_c, as shown by

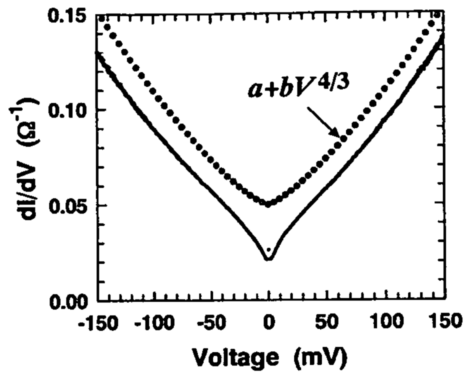

Fig. 5. Differential conductance versus Voltage characteristics at 4.2 K observed for an IEJ with I_c of 0.03 mA and R_n of 40 Ω at 4.2 K. The dotted line represents $V^{4/3}$ dependence for reference.

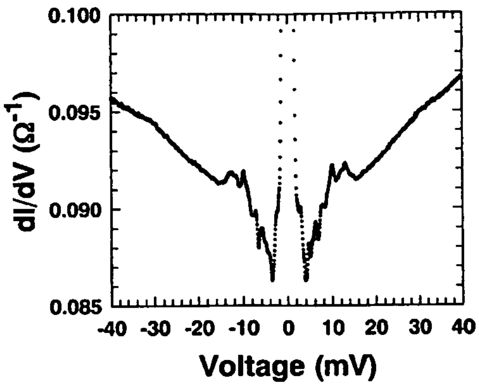

Fig. 6. Differential conductance versus voltage characteristics observed for an IEJ with an R_n of around 10 Ω.

group A. On the other hand, junctions with an I_c exceeding 3 mA exhibited nearly $(1-T/T_c)^{3/2}$ dependence (group B). It is known that Josephson junctions with thin normal conducting or reduced-T_c layers on both sides of a rigid interface barrier with low transparency exhibit $(1-T/T_c)^2$ dependence, and this dependence changes to $(1-T/T_c)^{3/2}$ when the normal conducting layer on one side of the interface disappears [5]. Such a picture seems to be consistent with our experimental data.

Fig. 5 shows the differential conductance versus voltage ($dI/dV - V$) characteristics observed for an IEJ with an I_c of 0.03 mA and an R_n of 40 Ω at 4.2 K. The dI/dV profile can be characterized by a slightly nonlinear increase in the conductance at high voltages, and a symmetrical dip structure around zero voltage. We found that the nonlinear behavior at high voltages was essentially independent of temperature, and fit well by $V^{4/3}$, as shown by the dotted line in the figure. This indicates that inelastic tunneling via two localized states in the barrier plays a part in the quasiparticle transport at high voltages [6]. IEJ's with R_n far exceeding 10 Ω exhibited similar characteristics. Thus, it seems reasonable to think that IEJ's with a high normal resistance have an insulator barrier with a high density of localized states in it.

It is well recognized that, in tunnel junctions with a barrier containing localized states, resonant tunneling through the localized states often dominates the quasiparticle transport at low voltages, while Cooper pairs can transfer only by direct tunneling [7]. The existence of different transport channels for quasiparticles and Cooper pairs manifests itself in the different tunnel barrier thickness dependences of I_c and R_n, resulting in a peculiar relationship between I_c and R_n as R_n is proportional to I_c^{-p} with p of less than 1. In the case where the quasiparticle current is dominated entirely by resonant tunneling, p is 0.5. This value becomes smaller when a contribution from inelastic processes via more than two localized states becomes noticeable. Generally, inelastic tunneling via n localized states is known to give $p = (n+1)^{-1}$, and the relative importance of inelastic processes increases as the tunnel barrier thickness increases [6]. Thus, we can expect a gradual decrease in p with an increase in the junction resistance. This is exactly what we saw in Fig. 3 for our IEJ's with R_n far larger than 10 Ω.

The origin of the symmetrical dip around zero voltage is not clear at present. A possible explanation may be an off-site Coulomb charging energy in the resonant tunneling process [8].

The dI/dV profiles of IEJ's having an R_n of around 10 Ω or less differ considerably from those of higher-resistance junctions. Fig. 6 depicts the dI/dV profile at 4.2 K observed for a junction with an R_n of slightly larger than 10 Ω. We can see distinct fine structures in the profile below 15 mV, and also some anomaly around 30 mV. We confirmed that the structures, at least those below 15 mV, were reproducible among junctions, and were enhanced with decreasing R_n. We also noticed that the sharpness of the fine structures correlated with the I_c value of individual junctions, i.e., when we compared two junctions with similar R_n values, the junction with the higher I_c always exhibited more pronounced structures in its dI/dV profile. Another feature we found in our low-R_n junctions is that the differential conductance of junctions with an R_n of several ohms or higher increases as the voltage increases, while that of junctions with R_n of a few ohms shows the opposite behavior.

The seemingly intricate experimental data mentioned above can be understood by assuming two kinds of current transport channels coexisting in the junctions. We think that one of them carries the Josephson current, and is also responsible for the weak bump-like structure in I–V characteristics in magnetic fields, the fine structures in dI/dV profiles, and the negative coefficient of dI/dV versus V in high bias regions. Another channel is a resistive one which gives rise to a positive curvature in dI/dV versus V characteristics. This channel has little effect on the Josephson current other than providing a shunting resistor within a junction. If we assume that the relative dominance of these two transport channels varies with process conditions, we can then systematically explain the wide variety of junction characteristics observed for our IEJ's.

It has long been recognized that some superconducting microbridges exhibit peculiar characteristics similar to those of the first transport channel in the IEJ's we described above [9]. Klapwijk, Blonder, and Tinkham first pointed out the importance of the multiple Andreev reflection (MAR) process in such junctions, and demonstrated that the singularities in dI/dV profiles below the gap voltage (subharmonic gap structure, SGS) as well as the excess current at high voltages were the consequences of the MAR process [10].

The MAR process manifests itself most clearly as singularities in dI/dV profiles at voltages $V_n = 2\Delta/en$, $n = 1, 2, 3, \ldots$, where Δ is the superconducting gap of the junction electrodes. Unfortunately, the fine structures below 15 mV in our junctions shown in Fig. 6 do not permit such simple labeling of the singularities. Moreover, in most cases, we were not able to find reproducible structures at higher voltages, though the junction shown in Fig. 6 exhibits an exceptionally weak anomaly around 30 mV. Similar deviation from the simple MAR model has been reported for the singularities in dI/dV profiles of ramp-edge junctions with a PrBaCuO barrier [11]. In this case, the absence of regular periodicity in SGS has been ascribed to the existence of a reduced-T_c layer adjacent to the tunnel barrier. The presence of such reduced-T_c layers was confirmed for our IEJ's through the temperature dependence of I_c. According to the recent theoretical investigations, the proximity effect between the reduced-T_c layer and the superconducting electrode also smears out the SGS singularity at $V = 2\Delta/e$ [12], [13]. All these facts seem to support the picture that the singularities in the dI/dV profiles of our IEJ's originate from the MAR process.

It is natural to suppose that the resonant tunneling of quasiparticles via localized states in an insulative barrier, which is similar to that in high-resistance junctions, constitutes the resistive channel even in low-resistance junctions. We suppose that the tunneling region exists dispersively in the junction area without forming a continuous barrier in such junctions exhibiting the MAR process. The relative area occupied by the tunneling channel as well as the resonant tunneling probability of quasiparticles would vary with process conditions, resulting in a variation in R_n by a factor of 3–4 even for junctions with similar I_c values.

The situation of junctions with a lower R_n is more complicated. We confirmed that these junctions exhibited a substantial amount of excess currents as well as peculiar singularities in their dI/dV profiles, indicating that MAR plays a significant role. The presence of normal conducting or reduced-T_c layers adjacent to the junction interface and parallel conduction through tunneling paths similar to those in higher-R_n junctions was also inferred from experiments. These results indicate that IEJ's with a high J_c and a low R_n, and thus of particular importance for SFQ circuit applications, are inhomogeneous in terms of their microscopic structures. At present, we do not have sufficient data to discuss to what extent this inherent inhomogeneity in junction structure restricts the achievable minimum 1σ-spread in I_c. Further detailed investigations are definitely required to answer this question.

IV. Summary

We have shown experimental evidence of two different transport channels in interface-engineered junctions, of which the relative dominance varies with the process conditions. We confirmed that elastic and inelastic tunneling via localized states embedded in an insulator dominate the quasiparticle transport in junctions with R_n far exceeding 10^{-7} Ωcm^2, indicating that these junctions are essentially tunnel junctions. Although we do not have concrete evidence, it seems rational to think that direct tunneling of Cooper pairs through the barrier is responsible for the Josephson current in these junctions.

References

[1] B. H. Moeckly and K. Char, "Properties of interface-engineered high-Tc Josephson junctions," *Appl. Phys. Lett.*, vol. 71, pp. 2526–2528, Oct. 1997.

[2] Y. Soutome *et al.*, "Investigations of ramp-type Josephson junctions with surface modified barriers," *IEEE Trans. Appl. Supercond.*, vol. 11, pp. 163–166, March 2001.

[3] H. Katsuno, S. Inoue, T. Nagano, and J. Yoshida, "Characteristics of interface-engineered Josephson junctions using a $YbBa_2Cu_3O_y$ counter-electrode layer," *Appl. Phys. Lett.*, vol. 79, pp. 4189–4191, Dec. 2001.

[4] J. P. Sydow, M. Berninger, R. A. Buhrman, and B. H. Moeckly, "Effects of oxygen content on YBCO Josephson junction structures," *IEEE Trans. Appl. Supercond.*, vol. 9, pp. 2993–2996, June 1999.

[5] A. A. Golubov *et al.*, "Proximity effect in superconductor-insulator-superconductor Josephson junctions: Theory and experiments," *Phys. Rev. B*, vol. 51, pp. 1073–1089, Jan. 1995.

[6] L. I. Glazman and K. A. Matveev, "Inelastic tunneling across thin amorphous films," *Sov. Phys. JETP*, vol. 67, pp. 1276–1282, June 1988.

[7] R. Gross *et al.*, "Physics and technology of high temperature superconducting Josephson junctions," *IEEE Trans. Appl. Supercond.*, vol. 7, pp. 2929–2935, June 1997.

[8] J. Halbritter, "Pair weakening and tunnel channels at cuprate interfaces," *Phys. Rev.*, vol. 46, pp. 14 861–14 871, Dec. 1992.

[9] P. E. Lindelof, "Superconducting microbridges exhibiting Josephson properties," *Rep. Prog. Phys.*, vol. 44, pp. 949–1026, Sept. 1981.

[10] T. M. Klapwijk, G. E. Blonder, and M. Tinkham, "Explanation of subharmonic energy gap structures in superconducting contacts," *Physica*, vol. 109&110B+C, pp. 1657–1664, July 1982.

[11] A. Engelhardt, R. Dittmann, and A. I. Braginski, "Subgap conductance features of $Yba_2Cu_3O_{7-\delta}$ edge Josephson junctions," *Phys. Rev. B*, vol. 59, pp. 3815–3822, Feb. 1999.

[12] B. A. Aminov, A. A. Golubov, and M. Yu Kupriyanov, "Quasiparticle current in ballistic constrictions with finite transparencies of interfaces," *Phys. Rev. B*, vol. 53, pp. 365–373, Jan. 1996.

[13] A. V. Zaitsev and D. V. Averin, "Theory of ac Josephson effect in superconducting constriction," *Phys. Rev. Lett.*, vol. 80, pp. 3602–3605, April 1998.